Supporting Information

A sequential light-harvesting system with thermosensitive colorimetric emission in both aqueous solution and hydrogel

Lu Tang,[a] Zhiying Wu,[a] Qiaona Zhang,[a] Qiulin Hu,[b] Xiaoman Dang,[a] Fengyao Cui,[a] Long Tang*[a,b] and Tangxin Xiao*[a]

[a]Jiangsu Key Laboratory of Advanced Catalytic Materials and Technology, School of Petrochemical Engineering, Changzhou University, Changzhou 213164, China, E-mail: xiaotangxin@cczu.edu.cn

[b]School of Pharmacy & School of Biological and Food Engineering, Changzhou University, Changzhou 213164, China, E-mail: tanglong@cczu.edu.cn

Table of contents

1. Materials, methods, and abbreviations

General

All chemicals, reagents and solvents were purchased from commercial suppliers and used, unless otherwise stated, without further purification. If needed, solvents were dried according to literature procedures. All yields were given as isolated yields. Compound **1**[S1] and **2**[S2] were synthesized according to literature.

NMR spectroscopy

The ^{1}H NMR and ^{13}C NMR spectra were recorded with a Bruker AVANCE III (300 MHz) spectrometer and calibrated against the residual proton signal or natural abundance carbon resonance of the used deuterated solvent from tetramethylsilane (TMS) as the internal standard. The chemical shifts δ are indicated in ppm and the coupling constants J in Hz. The multiplicities are given as s (singlet), m (multiplet), and br (broad).

Mass spectrometry

High-resolution electrospray ionization mass spectra (HR-ESI-MS) were recorded on an Agilent Technologies 6540 UHD Accurate-Mass.

Dynamic light scattering (DLS)

DLS measurements were carried out on a Brookhaven BI-9000AT system, equipped with a 200 mW polarized laser source (λ = 514 nm) at a scattering angle of 90°. All samples were prepared according to the corresponding procedures mentioned above.

Transmission electron microscope (TEM)

TEM investigations were carried out on a JEM-2100 instrument.

UV-vis spectroscopy

The UV-vis absorption spectra were measured on a Shimadzu UV-vis Spectrophotometer (UV-1900i).

Fluorescence spectroscopy

Fluorescence measurements were performed on an Agilent Cary Eclipse spectrofluorometer.

Fluorescence lifetimes

The fluorescence lifetimes were measured employing time correlated single photon counting on a FLS980 instrument with a pulsed xenon lamp. Analysis of fluorescence decay curves were subjected to fit by a bi-exponential decay.

Quantum yields

The quantum yields were carried out on a FLS980 instrument with the integrating sphere.

CIE coordinates

The CIE (Commission Internationale de l'Eclairage) 1931 coordinates were calculated with the method of color matching functions.

Abbreviations

CAC = critical aggregation concentration; NPs = nanoparticles; DCM = dichloromethane; MeOH = methanol; M = mol/L.

2. Synthesis of TPEO

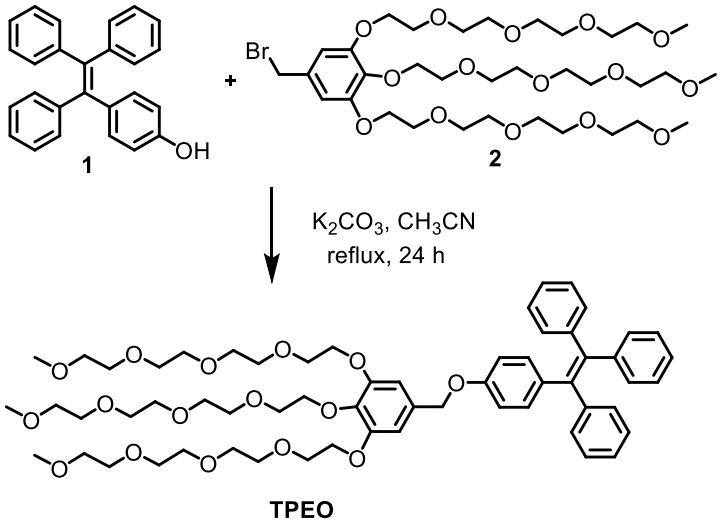

Scheme S1. Synthetic route of **TPEO**. Compound **1**[S1] and compound **2**[S2] were synthesized according to the literature procedures.

Synthesis of compound TPEO

To a flask equipped with a magnetic stirrer, K_2CO_3 (0.30 g, 2.2 mmol), compound **1** (0.50 g, 1.4 mmol) and acetonitrile (15 mL) were charged under N_2 atmosphere. Subsequently, to the flask an acetonitrile (5 mL) solution of compound **2** (1.25 g, 1.6 mmol) was dropped slowly. The obtained mixture was refluxed for 24 h. Then the reaction mixture was cooled down to room temperature and was concentrated under reduced pressure. The crude product was purified by silica gel column chromatography (DCM : MeOH = 50 : 1, v/v) to afford compound TPEO as a viscous oil (0.73 g, 0.7 mmol, 50%). ^{1}H NMR (300 MHz, DMSO-d_6, δ): 7.18-7.06 (m, 9H, Ar-*H*), 7.02-6.91 (m, 6H, Ar-*H*), 6.90-6.83 (m, 2H, Ar-*H*), 6.80-6.70 (m, 4H, Ar-*H*), 4.88 (s, 2H, -OC*H*$_2$-Ar), 4.12-4.04 (m, 4H, -C*H*$_2$-), 4.01 (t, *J* = 4.7 Hz, 2H, -C*H*$_2$-), 3.76-3.69 (m, 4H, -C*H*$_2$-), 3.67 (t, *J* = 4.7 Hz, 2H, -C*H*$_2$-), 3.62-3.55 (m, 6H, -C*H*$_2$-), 3.55-3.45 (m, 24H, -C*H*$_2$-), 3.45-3.37 (m, 6H, -C*H*$_2$-), 3.26-3.18 (m, 9H, -OC*H*$_3$). ^{13}C NMR (75 MHz, $CDCl_3$, δ): 157.22, 152.72, 143.99, 143.93, 140.45, 140.18, 138.07, 136.46, 132.56, 132.38, 131.38, 131.34, 127.72, 127.60, 126.37, 126.28, 113.90, 107.19, 72.32, 71.93, 70.81, 70.66, 70.60, 70.51, 69.89, 69.72, 68.84, 59.03. HRMS (ESI) *m/z*: $[M + NH_4^+]^+$ calcd for $[C_{60}H_{84}NO_{16}]^+$ = 1074.5785; found 1074.5762; $[M + Na^+]^+$ calcd for $[C_{60}H_{80}NaO_{16}]^+$ = 1079.5339; found 1079.5312.

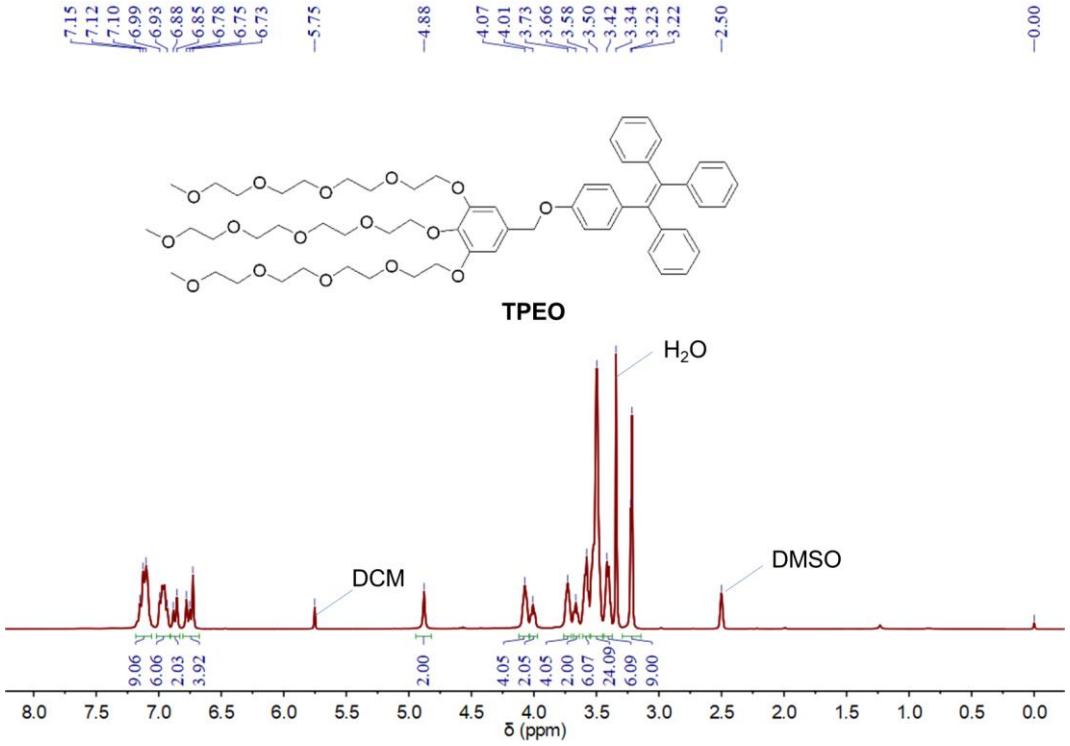

Fig. S1. ^{1}H NMR spectrum (300 MHz, DMSO-d_6, 298 K) of **TPEO**.

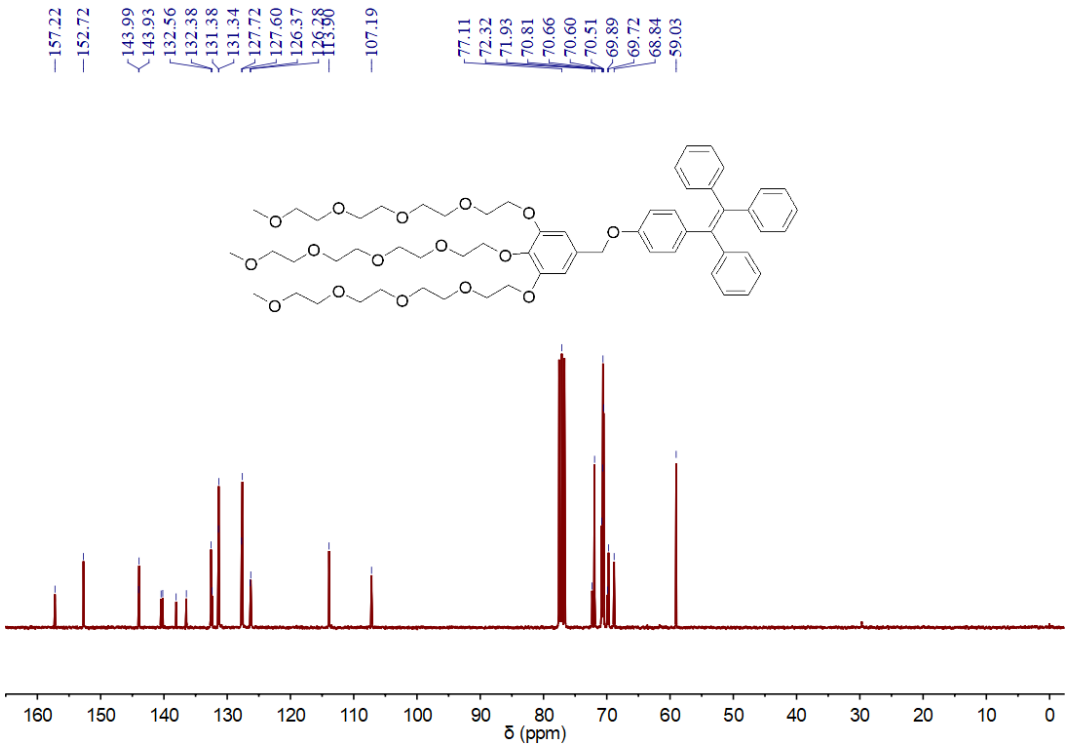

Fig. S2. ^{13}C NMR spectrum (75 MHz, $CDCl_3$, 298 K) of **TPEO**.

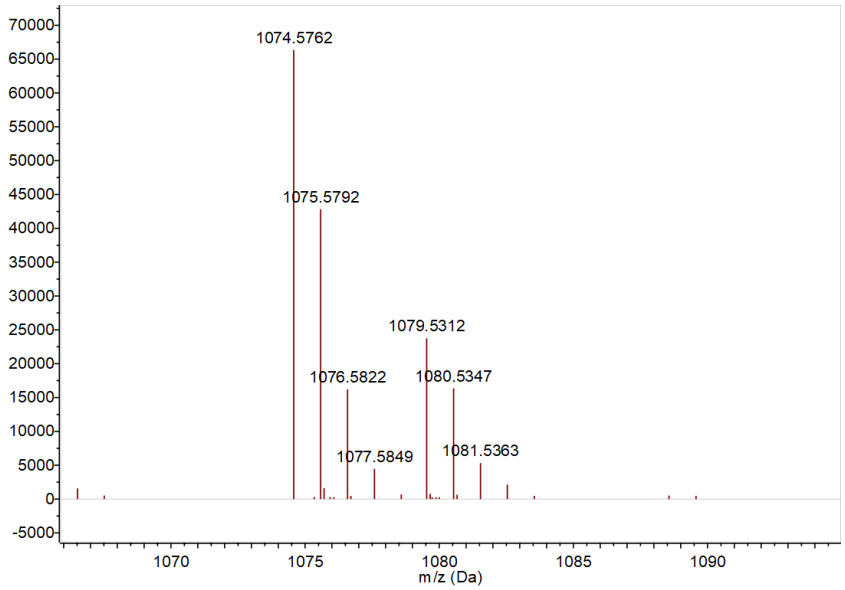

Fig. S3. HR-MS (ESI, positive mode, CH_3OH) of **TPEO**.

3. Critical aggregation concentration of TPEO in water

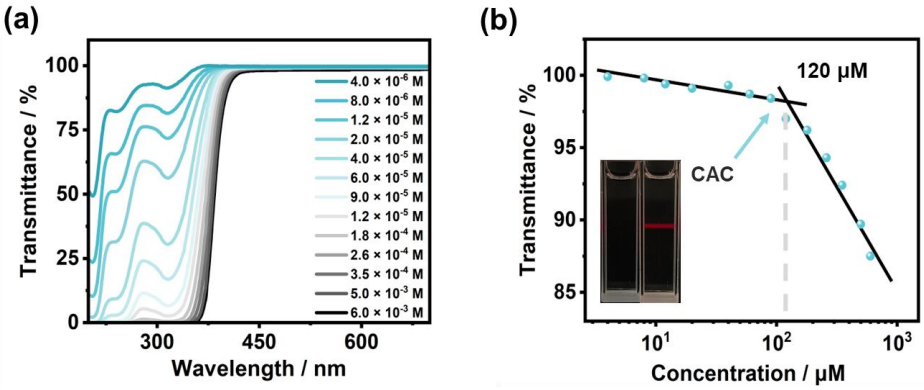

Fig. S4. (a) Concentration-dependent full-wavelength transmittance spectra of **TPEO** in water. (b) Concentration-dependent optical transmittance of **TPEO** at 400 nm, insets: Tyndall effect of **TPEO** in water at 20 μM (left) and 1000 μM (right).

Full-wavelength transmittance experiments were conducted on **TPEO** aqueous solutions with different concentrations from 4 to 6000 μM (Fig. S4a). The results showed that the transmittance decreased as the concentration increased. In order to quantitatively analyze the decrease process of transmittance, the transmittance values of **TPEO** at 400 nm at different concentrations are plotted in Fig. S4b, showing that there is a turning point at 120 μM, which is the critical aggregation concentration (CAC). As the concentration increases, the optical transmittance first decreases slowly, and then decreases sharply after passing the CAC point. This is because **TPEO** self-assembled into a large number of dispersed nanoaggregates at high concentrations, which greatly reduces the optical transmittance of the solution. Furthermore, the Tyndall effect was clearly observed in 1000 μM **TPEO** aqueous solution, but no similar effect was found in a low-concentration solution (20 μM), again indicating the formation of abundant nanoaggregates above the CAC (Fig. S4b, inset).

4. Fluorescence of TPEO in DMSO/H_2O mixed solvent

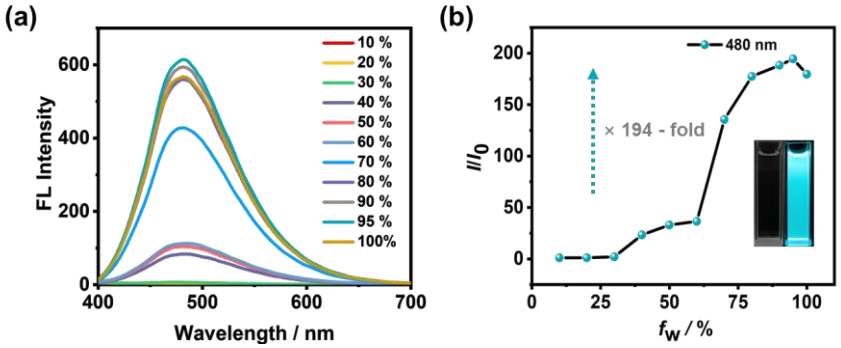

Fig. S5. (a) Fluorescence spectra of **TPEO** (2.0×10^{-4} M) in DMSO/water mixtures with different water fractions (λ_{ex} = 355 nm). (b) Plot of I/I_0 value versus the water fraction (f_w). I_0 is fluorescence intensity of **TPEO** in pure DMSO.

Based on the fact that **TPEO** forms nano-assemblies in the aqueous phase, and considering that TPE is an AIE group, the fluorescence properties of **TPEO** were further tested. For **TPEO**, DMSO is a good solvent and can dissolve it well. As shown in Fig. S5b (inset), **TPEO** in pure DMSO shows no fluorescence emission due to the free intramolecular motion of the TPE groups. In stark contrast, bright cyan fluorescence from **TPEO** was observed in pure water, which can be ascribed to the extremely restricted intramolecular motion of TPE in well-ordered nanoparticles. As shown in Fig. S5a, the fluorescence (FL) intensity of **TPEO** in DMSO/H_2O mixed solvent increases with the increase of water content (f_w). The fluorescence intensity increased 194 times during this process (Fig. S5b), signifying that **TPEO** is an excellent AIE molecule.

5. DLS and TEM measurements

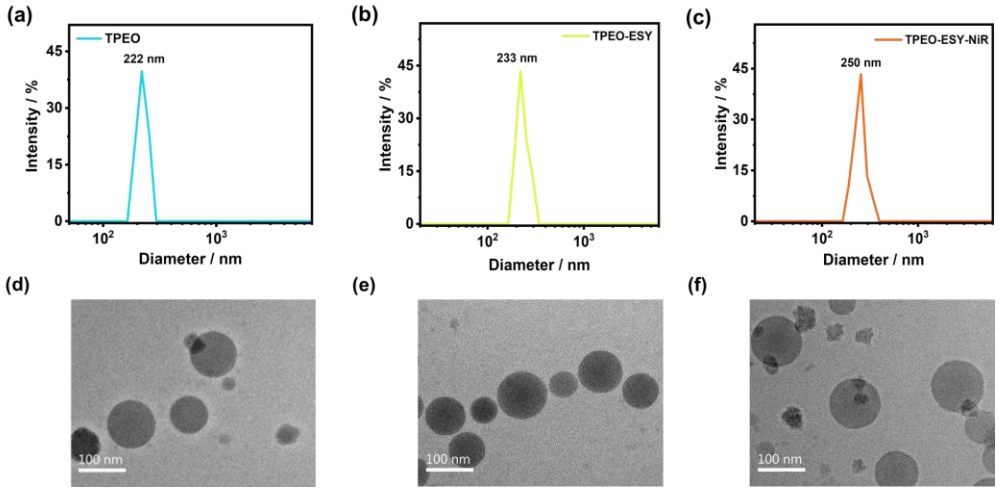

Fig. S6. DLS data of **TPEO** NPs (a), **TPEO-ESY** NPs (b), and **TPEO-ESY-NiR** NPs (c). TEM images of **TPEO** NPs (d), **TPEO-ESY** NPs (e), and **TPEO-ESY-NiR** NPs (f).

6. Temperature-responsive fluorescence emission

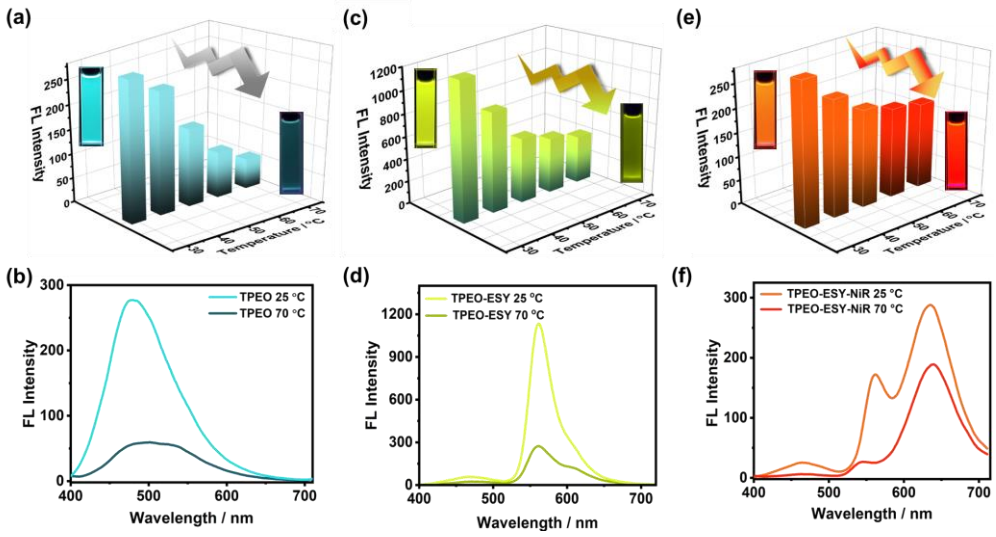

Fig. S7. (a) Histogram of fluorescence intensity of **TPEO** at 480 nm as a function of temperature, inset: fluorescent photo of **TPEO** at 25.0 ℃ (left) and 70.0 ℃ (right). (b) Fluorescence spectra of **TPEO** in water at 25.0 ℃ and 70.0 ℃, respectively. (c) Histogram of fluorescence intensity of **TPEO-ESY** at 560 nm as a function of temperature, inset: fluorescent photo of **TPEO-ESY** at 25.0 ℃ (left) and 70.0 ℃ (right). (d) Fluorescence spectra of **TPEO-ESY** in water at 25.0 ℃ and 70.0 ℃, respectively (D/A1 = 25/1). (e) Histogram of fluorescence intensity of **TPEO-ESY-NiR** at 630 nm as a function of temperature, inset: fluorescent photo of **TPEO-ESY-NiR** at 25.0 ℃ (left) and 70.0 ℃ (right). (f) Fluorescence spectra of **TPEO-ESY-NiR** in water at 25.0 ℃ and 70.0 ℃, respectively (D/A1/A2 = 1000/40/40). [**TPEO**] = 2.0×10^{-4} M.

Considering the impact of the thermal response characteristics of **TPEO** on its self-assembly process, the fluorescence emission of **TPEO** based on the AIE mechanism may also be sensitive to temperature. Therefore, the fluorescence response of **TPEO** to temperature was further studied. When the temperature was increased from 30.0 to 70.0 °C, the emission intensity of **TPEO** showed a gradual decrease trend (Fig. S7a and S7b). When the solution of **TPEO** was at room temperature, the molecules form well-organized nanoparticles, in which the TPE groups were packed together tightly, leading to a strong emission due to AIE. Conversely, when the temperature increases, these tightly packed TPE units become loose, resulting in reduced AIE and weakened fluorescence. It is worth noting that this temperature-responsive fluorescence weakening process of **TPEO** is reversible, and the fluorescence can be quickly restored after cooling to room temperature.

7. Fluorescence quantum yield and lifetime measurements

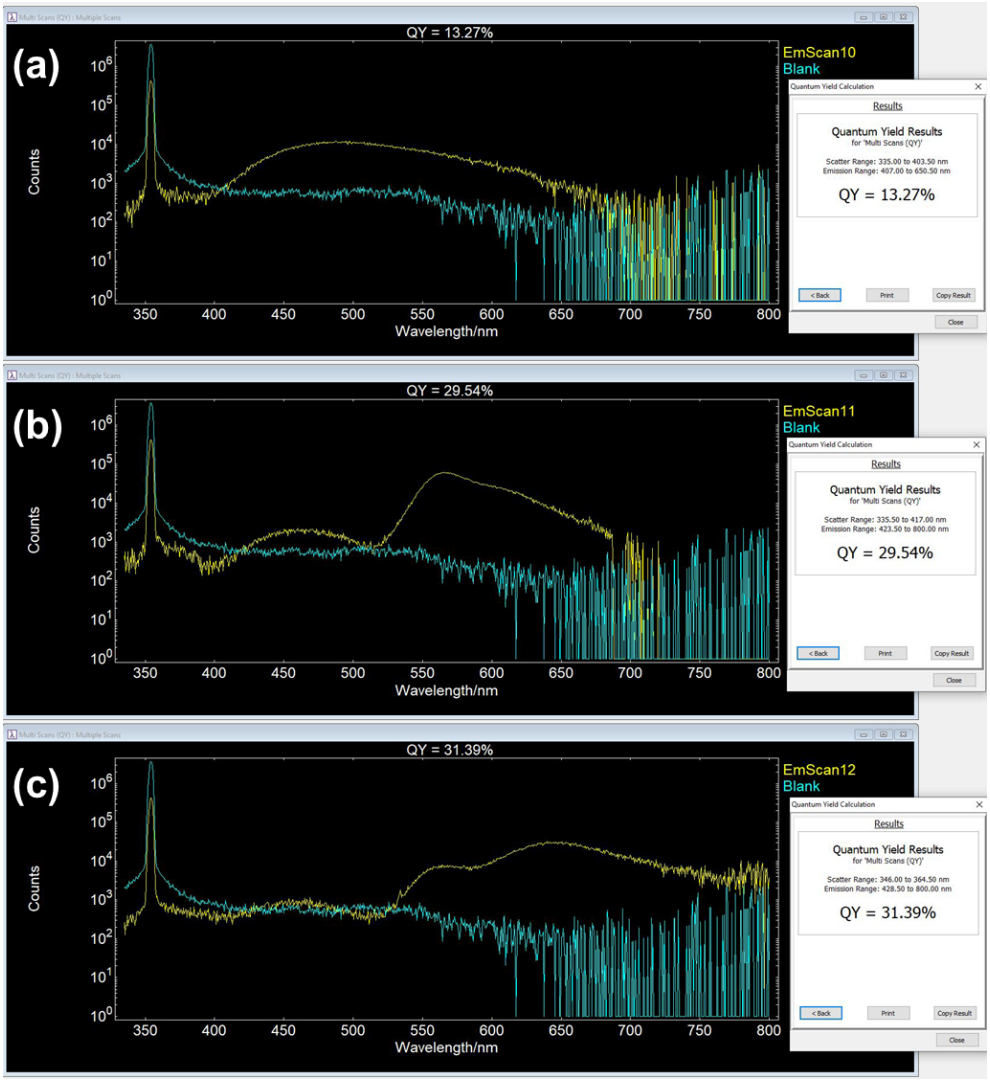

Fig. S8. Absolute fluorescence quantum yields ($\Phi_{f(abs)}$) of (a) **TPEO**, (b) **TPEO-ESY** (**TPEO**/**ESY** = 25/1), (c) **TPEO-ESY-NiR** (**TPEO**/**ESY**/**NiR** = 1000/40/40) upon excitation at 355 nm. [**TPEO**] = 2.0×10^{-4} M, [**ESY**] = 8.0×10^{-6} M, [**NiR**] = 8.0×10^{-6} M.

Table S1. Fluorescence quantum yields data of **TPEO**, **TPEO-ESY**, and **TPEO-ESY-NiR** NPs.

Sample	**Fluorescence quantum yields ($\Phi_{f(abs)}$)**
TPEO	13.27%
TPEO-ESY (**TPEO**: **ESY** = 25: 1)	29.54%
TPEO-ESY-NiR (**TPEO**: **ESY**: **NiR** = 1000: 40: 40)	31.39%

Table S2. Fluorescence lifetimes of **TPEO** and **TPEO-ESY** monitored at 480 nm. [**TPEO**] = 2.0 × 10^{-4} M, [**ESY**] = 8.0 × 10^{-6} M, respectively.

Sample	τ_1/ns	RW1%	τ_2/ns	RW2%	τ/ns	χ^2
TPEO	1.10	33.02	4.03	66.98	3.06	1.0750
TPEO-ESY (**TPEO**: **ESY** = 25: 1)	0.89	42.21	3.81	57.79	2.58	1.0105

Table S3. Fluorescence lifetimes of **TPEO-ESY** and **TPEO-ESY-NiR** monitored at 560 nm. [**TPEO**] = 2.0 × 10^{-4} M, [**ESY**] = 8.0 × 10^{-6} M, [**NiR**] = 8.0 × 10^{-6} M, respectively.

Sample	τ_1	RW1%	τ_2	RW2%	τ/ns	χ^2
TPEO-ESY (**TPEO**: **ESY** = 25: 1)	2.26	23.52%	3.55	76.48%	3.24	1.0641
TPEO-ESY-NiR (**TPEO**: **ESY**: **NiR** = 1000: 40: 40)	0.75	58.21%	3.45	41.79%	1.88	1.0614

8. Energy-transfer efficiency calculation

(1) Energy-transfer efficiency of the first-step FRET

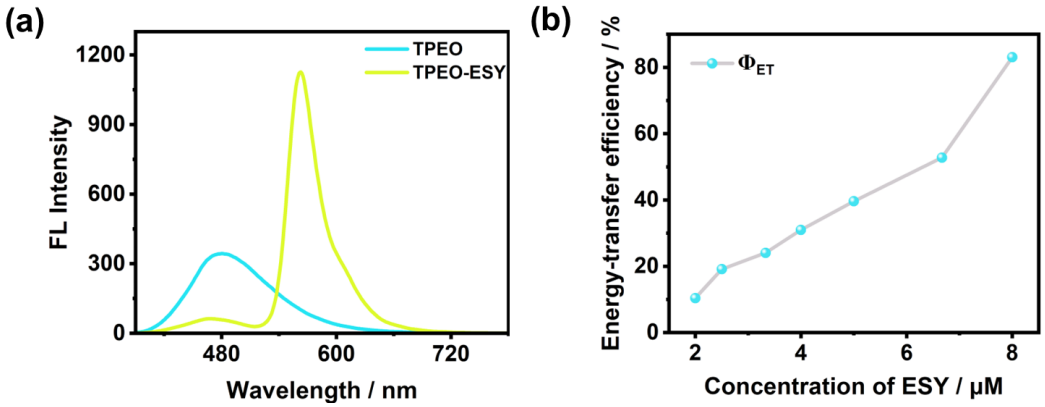

Fig. S9. Fluorescence spectra of **TPEO** and **TPEO-ESY** upon excitation at 355 nm. [**TPEO**] = 2.0 × 10^{-4} M, [**ESY**] = 8.0 × 10^{-6} M, respectively.

Energy-transfer efficiency (Φ_{ET}) was calculated from fluorescence spectra through the equation S1[S3]:

$$\Phi_{ET} = 1 - I_{DA}/I_D \text{ (eq. S1)}$$

Where I_{DA} and I_D are the fluorescence intensities of TPEO-ESY (donor-acceptor assembly) and TPEO (donor) at 480 nm when excited at 355 nm, respectively.

Table S4. Energy-transfer efficiency of the first-step FRET with different **TPEO**/**ESY** ratio.

Sample	Concentration, respectively	Energy-transfer efficiency (Φ_{ET})
TPEO-ESY (**TPEO-ESY** = 25:1)	[**TPEO**] = 2.0×10^{-4} M [**ESY**] = 8.0×10^{-6} M	83.04%
TPEO-ESY (**TPEO-ESY** = 30:1)	[**TPEO**] = 2.0×10^{-4} M [**ESY**] = 6.7×10^{-6} M	52.76%
TPEO-ESY (**TPEO-ESY** = 40:1)	[**TPEO**] = 2.0×10^{-4} M [**ESY**] = 5.0×10^{-6} M	39.59%
TPEO-ESY (**TPEO-ESY** = 50:1)	[**TPEO**] = 2.0×10^{-4} M [**ESY**] = 4.0×10^{-6} M	30.98%
TPEO-ESY (**TEPO-ESY** = 60:1)	[**TPEO**] = 2.0×10^{-4} M [**ESY**] = 3.3×10^{-6} M	24.04%
TPEO-ESY (**TPEO-ESY** = 80:1)	[**TPEO**] = 2.0×10^{-4} M [**ESY**] = 2.5×10^{-6} M	19.13%
TPEO-ESY (**TPEO-ESY** = 100:1)	[**TPEO**] = 2.0×10^{-4} M [**ESY**] = 2.0×10^{-6} M	10.40%

(2) Energy-transfer efficiency of the second-step FRET

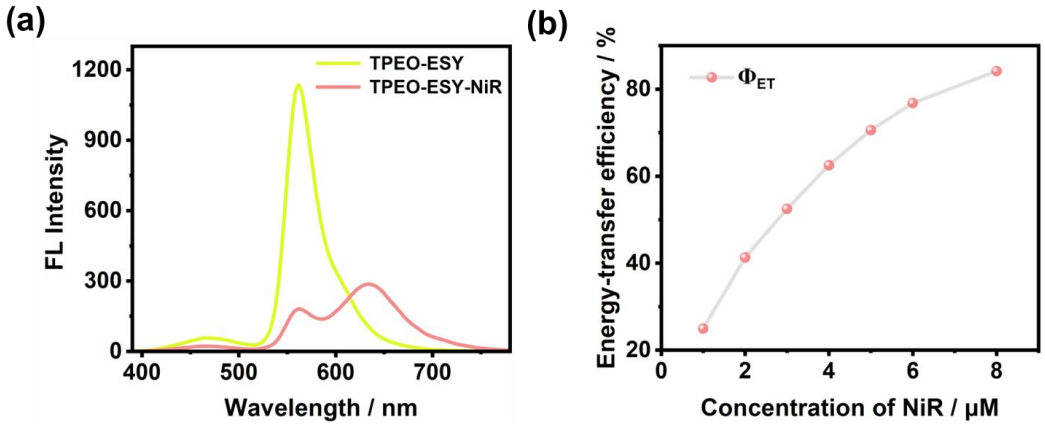

Fig. S10. Fluorescence spectra of **TPEO-ESY** and **TPEO-ESY-NiR** upon excitation at 355 nm. [**TPEO**] = 2.0×10^{-4} M, [**ESY**] = 8.0×10^{-6} M, [**NiR**] = 8.0×10^{-6} M, respectively.

Energy-transfer efficiency (Φ_{ET}) of the second-step FRET was calculated from fluorescence spectra through the equation S1[S3]:

$$\Phi_{ET} = 1 - I_{DA}/I_D$$

Where I_{DA} and I_D are the fluorescence intensities of **TPEO-ESY-NiR** and **TPEO-ESY** at 560 nm when excited at 355 nm, respectively.

Table S5. Energy-transfer efficiency of the second-step FRET with different **TPEO**/**ESY**/**NiR** ratio.

Sample	Concentration, respectively	Energy-transfer efficiency (Φ_{ET})
TPEO-ESY-NiR (**TPEO-ESY-NiR** = 1000:40:40)	[**TPEO**] = 2.0 × 10^{-4} M [**ESY**] = 8.0 × 10^{-6} M [**NiR**] = 8.0 × 10^{-6} M	84.14%
TPEO-ESY-NiR (**TPEO-ESY-NiR** = 1000:40:30)	[**TPEO**] = 2.0 × 10^{-4} M [**ESY**] = 8.0 × 10^{-6} M [**NiR**] = 6.0 × 10^{-6} M	76.80%
TPEO-ESY-NiR (**TPEO-ESY-NiR** = 1000:40:25)	[**TPEO**] = 2.0 × 10^{-4} M [**ESY**] = 8.0 × 10^{-6} M [**NiR**] = 5.0 × 10^{-6} M	70.58%
TPEO-ESY-NiR (**TPEO-ESY-NiR** = 1000:40:20)	[**TPEO**] = 2.0 × 10^{-4} M [**ESY**] = 8.0 × 10^{-6} M [**NiR**] = 4.0 × 10^{-6} M	62.51%
TPEO-ESY-NiR (**TPEO-ESY-NiR** = 1000:40:15)	[**TPEO**] = 2.0 × 10^{-4} M [**ESY**] = 8.0 × 10^{-6} M [**NiR**] = 3.0 × 10^{-6} M	52.49%
TPEO-ESY-NiR (**TPEO-ESY-NiR** = 1000:40:10)	[**TPEO**] = 2.0 × 10^{-4} M [**ESY**] = 8.0 × 10^{-6} M [**NiR**] = 2.0 × 10^{-6} M	41.30%
TPEO-ESY-NiR (**TPEO-ESY-NiR** = 1000:40:5)	[**TPEO**] = 2.0 × 10^{-4} M [**ESY**] = 8.0 × 10^{-6} M [**NiR**] = 1.0 × 10^{-6} M	24.96%

9. Tunable white light emission

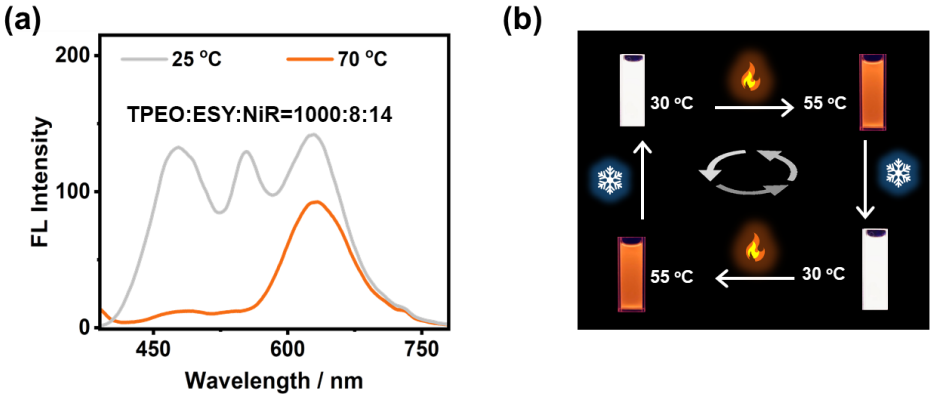

Fig. S11. (a) Fluorescence spectra of **TPEO-ESY-NiR** with D/A1/A2 = 1000/8/14 at 25.0 °C and 70.0 °C ([**TPEO**] = 2.0 × 10^{-4} M). (b) Fluorescence cycle image of tunable white-light emission between 30.0 °C and 55.0 °C.

10. Demonstration of hydrogel production process

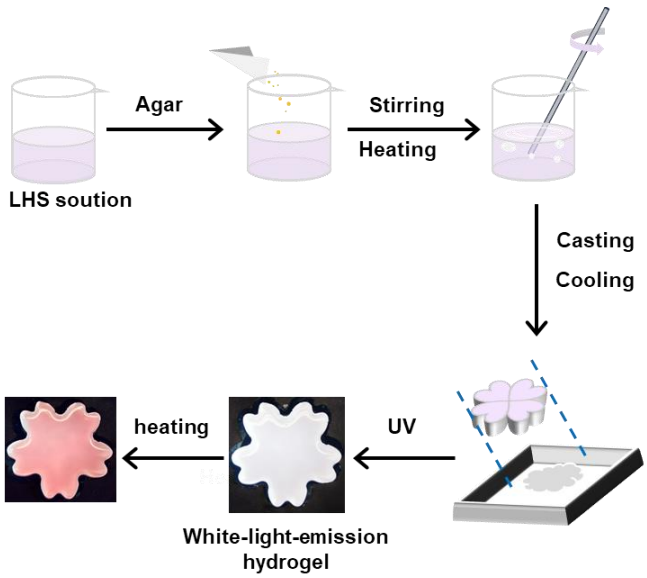

Figure S12. Schematic representation of the preparation of hydrogels with temperature-responsive white-light emission.

Preparation of temperature-responsive hydrogels. Firstly, a white-light emitting LHS solution was prepared. Aqueous solution of **TPEO** (D, 160 μL, 5 mM), DMSO solution of **ESY** (A1, 12.8 μL, 0.5 mM), and DMSO solution of **NiR** (A2, 22.4 μL, 0.5 mM) were sequentially added to deionized water (3804.8 μL) and ultrasonicated for 5 min to afford a white-light emitting solution (4 mL) with a molar ratio of D/A1/A2 = 1000:8:14. Secondly, agar powder (40 mg) was added to the above solution. After heating, stirring, and cooling, the solution was poured into the mold and left to stand for 30 min. After the gel was formed, it was demolded to produce a temperature-responsive white light-emitting hydrogel with a specific shape

11. References

[S1] X. Xue, Y. Zhao, L. Dai, X. Zhang, X. Hao, C. Zhang, S. Huo, J. Liu, C. Liu, A. Kumar, W.-Q. Chen, G. Zou, X.-J. Liang, *Adv. Mater.* **2014**, 26, 712.

[S2] M. D. Tzirakis, M. N. Alberti, H. Weissman, B. Rybtchinski, F. Diederich, *Chem. Eur. J.* **2014**, 20, 16070.

[S3] M. Hao, G. Sun, M. Zuo, Z. Xu, Y. Chen, X. Y. Hu, L. Wang, *Angew. Chem. Int. Ed.* **2020**, 59, 10095.